Acta Cryst E CRYSTALLOGRAPHIC COMMUNICATIONS

ISSN 2056-9890

Crystal structure of *catena*-poly[2-bromoethylammonium [tin(II)-tri-μ-bromido]]

Valeriia M. Ovdenko,[a]* Mircea-Odin Apostu,[b] Irina A. Golenya,[a] Anna Yu. Myronenko[a] and Il'ya A. Gural'skiy[a]

[a]Department of Chemistry, Taras Shevchenko National University of Kyiv, Volodymyrska St. 64/13, Kyiv 01601, Ukraine, and [b]Department of Chemistry, Faculty of Chemistry, Al. I. Cuza University of Iasi, 11 Carol I Blvd, Iasi 700506, Romania. *Correspondence e-mail: valeryovdenko@knu.ua

Received 28 April 2026
Accepted 9 June 2026

Edited by M. Weil, Vienna University of Technology, Austria

Keywords: crystal structure; hybrid perovskite like compound; tin(II); polymeric chain.

CCDC reference: 2560931

Supporting information: this article has supporting information at journals.iucr.org/e

In the structure of the title salt, $\{(C_2H_7BrN)[SnBr_3]\}_n$, the tin(II)atom features a strongly distorted octahedral environment ensured by six bromido ligands. By face-sharing, these $SnBr_6$ coordination octahedra are connected into polymeric chains, which propagate along the *b*-axis direction. Organic cations, stabilized in a *gauche* conformation, interleave the inorganic polymeric chains. Hydrogen bonds of the type N—H···Br between organic cations and inorganic chains create supramolecular layers parallel to the *ab* plane. These layers interact with each other thought weak C—H···Br contacts.

1. Chemical context

Hybrid organic–inorganic metal halides have emerged as an important class of semiconducting materials owing to their optical and electronic properties and their applicability in a wide range of optoelectronic devices, including solar cells, light-emitting diodes, photodetectors, and lasers (Zhang *et al.*, 2023). The archetypal halide perovskites adopt the general formula ABX_3, where A is a monovalent organic or inorganic cation, B is a divalent metal cation (commonly Pb^{2+} or Sn^{2+}), and X is a halide anion. In the corresponding crystal structures, corner-sharing BX_6 octahedra form an extended framework that is responsible for their favorable charge-transport and optical properties (Li *et al.*, 2017).

Despite their outstanding performance, the toxicity of lead has stimulated intense research into alternative compositions, among which tin-based halide perovskites are considered the most promising candidates due to their suitable band gaps, strong optical absorption, and high charge-carrier mobilities (Pitaro *et al.*, 2022). However, the use of Sn^{2+}-based systems can present specific challenges, including susceptibility to oxidation and a strong tendency toward structural diversity, which distinguishes them from their lead-based analogues. In particular, the stereochemically active $5s^2$ lone pair of Sn^{2+} often induces significant distortions of the coordination environment, leading to low-symmetry structures and a wide range of structural motifs (Stoumpos *et al.*, 2017; Sirenko *et al.*, 2024).

The periodicity of hybrid halide perovskites can be tuned by the size and functionality of the organic cations, giving rise to structures containing layers, chains, and discrete metal-halide octahedra (Zhou *et al.*, 2019). In such systems, the connectivity of the metal–halide octahedra – whether corner-, edge-, or face-sharing – plays a decisive role in determining their electronic structure and band gap. Reduced periodicity and non-corner-sharing connectivity generally lead to increased band

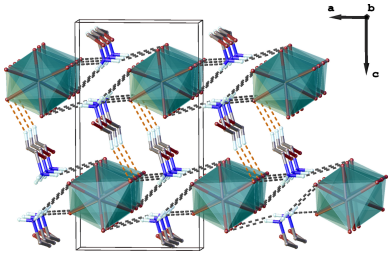

gaps, enhanced carrier localization, and pronounced excitonic effects. Consequently, zero-, mono- and diperiodic tin halides often exhibit distinct optical properties compared to their counterparts of the ABX_3 type.

Monoperiodic hybrid tin halides, in particular, have attracted growing attention due to their unique structural and physical properties. Their inorganic frameworks typically consist of chains of connected Sn–halide polyhedra, which may adopt different connectivity modes, including corner- and edge-sharing arrangements (Shi *et al.*, 2019; Spanopoulos *et al.*, 2020). These systems exhibit strong quantum confinement and enhanced electron–phonon coupling, often resulting in broadband emission that can originate from self-trapped excitons or defect-related states. Moreover, the structural flexibility of Sn^{2+} allows for the formation of highly distorted chains, which can further modulate the optical and electronic properties (Tao *et al.*, 2024).

The exploration of new tin(II) halide materials remains of considerable interest, particularly in relation to understanding structure–property relationships and expanding the library of perovskite-related architectures. In this context, the title compound formed unintentionally during the planned synthesis of aziridinium tin bromide (Kucheriv *et al.*, 2023) due to the high reactivity of aziridine, which can undergo ring-opening reactions in acidic media. The crystal structure of this new monoperiodic hybrid tin(II) bromide $(2\text{-BrC}_2\text{H}_4\text{NH}_3)[\text{SnBr}_3]$ features chains constructed from bromido-bridged Sn^{2+} cations, further contributing to the structural diversity of tin halide systems.

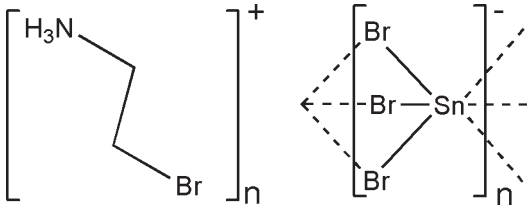

2. Structural commentary

The tin(II) cation features a strongly distorted octahedral coordination environment provided by six bromido ligands (Fig. 1, Table 1). These inorganic octahedra feature three short Sn—Br bonds and three long ones, the latter being shorter than the sum of the van der Waals radii of Sn and Br (4.00 Å; Mantina *et al.*, 2009). Such a coordination environment with asymmetric trigonal distortion of the octahedron created by three shorter-bonded halogen anions in combination with three longer Sn—X contacts is quite typical for Sn^{2+} and has been observed for similar perovskite-like structures (Fabini *et al.*, 2016). The octahedral distortion parameters of $[SnBr_6]$ are very high with $\Delta d = 1/6\Sigma(d_i - d)^2/d^2 = 0.0187$ (where d_i is one of six individual bond lengths in the octahedra and d is the mean Sn—Br bond length) and $\Sigma = \Sigma|90^\circ - \alpha| = 165.3^\circ$ (where α are the twelve *cis*-Br—Sn—Br angles). Alternatively, longer Sn—Br bonds can be considered as interionic contacts between pyramidal $[SnBr_3]$ moieties.

Table 1
Selected bond lengths (Å).

Sn1—Br1	2.7256 (10)	Br4*A*—C2*A*	1.921 (19)
Sn1—Br2	2.7228 (9)	Br4*B*—C2*B*	1.968 (19)
Sn1—Br3	2.6869 (11)	N1—C1	1.487 (11)
Sn1—Br2^{i}	3.3922 (9)	C1—C2*A*	1.40 (2)
Sn1—Br1^{ii}	3.4518 (10)	C1—C2*B*	1.49 (2)
Sn1—Br3^{ii}	3.7621 (9)		

Symmetry codes: (i) $-x+\frac{1}{2}, y+\frac{1}{2}, -z+\frac{1}{2}$; (ii) $-x+\frac{1}{2}, y-\frac{1}{2}, -z+\frac{1}{2}$.

The coordination octahedra in this structure are further connected in a face-sharing manner into chains extending parallel to the *b* axis (Fig. 2). The negative charge of inorganic chains is balanced by organic 2-bromoethylammonium cations, in which atoms Br4 and C2 are disordered in a nearly 1:1 ratio over two sets of sites. The observed bond lengths in the organic cation are within the expected ranges (Table 1), with the conformation being *gauche* with Br4*A*—C2*A*—C1—N1 and Br4*B*—C2*B*—C1—N1 torsion angles of 51 (2) and −58.2 (17)°, respectively.

3. Supramolecular features

Inorganic chains interact with organic counter-ions through a set of N—H···Br hydrogen bonds (Table 2, Figs. 2 and 3). Each protonated amino group creates three hydrogen bonds

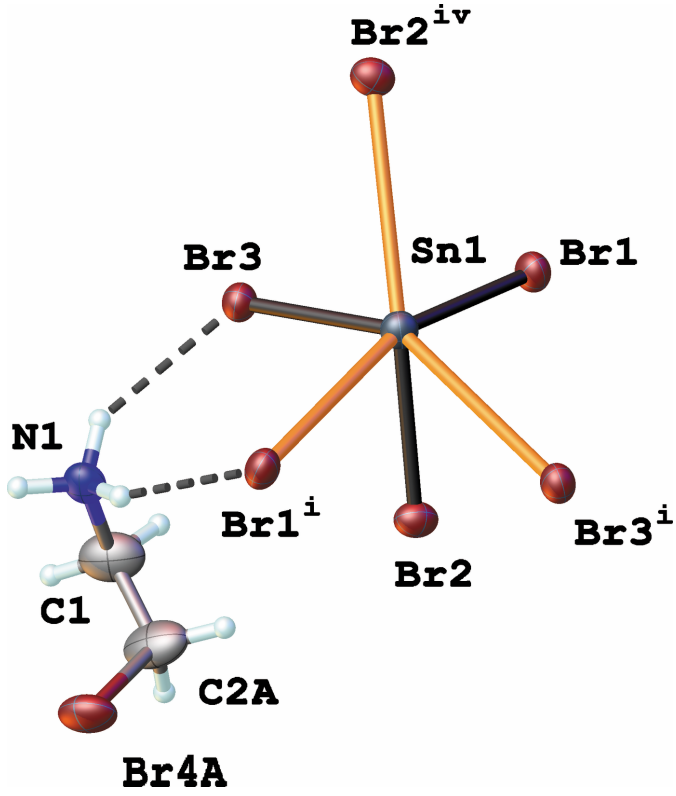

Figure 1
The distorted $[SnBr_6]$ coordination octahedron and the 2-bromoethylammonium cation in the title compound. Displacement ellipsoids are drawn at the 50% probability level. Short and long Sn—Br bonds are shown in black and orange, respectively. Only one part of the disordered organic cation is given for clarity; symmetry codes refer to Table 1.

Table 2
Hydrogen-bond geometry (Å, °).

D—H···A	D—H	H···A	D···A	D—H···A
N1—H1A···Br1^{ii}	0.91	2.66	3.507 (7)	156
N1—H1B···Br2^{iii}	0.91	2.62	3.491 (6)	160
N1—H1C···Br3	0.91	2.64	3.425 (6)	145
C1—H1BD···Br2^{iv}	0.99	2.94	3.882 (9)	159
C2A—H2AA···Br2	0.99	2.97	3.85 (3)	149

Symmetry codes: (ii) $-x+\frac{1}{2}, y-\frac{1}{2}, -z+\frac{1}{2}$; (iii) $x+1, y, z$; (iv) $-x+1, -y+1, -z+1$.

with bromide ions connecting two neighboring inorganic chains into supramolecular layers parallel to the *ab* plane. These supramolecular layers interact though weak C—H···Br interactions (Table 2, Fig. 2).

4. Database survey

A search of the Cambridge Structure Database (CSD; version 6.0, updated November 2025; Groom *et al.*, 2016) revealed four crystal structures containing tin halides in combination with 2-halogenoethylammonium cations. These compounds were considered because chemically similar 2-halogenoethylammonium cations often direct the structural set-up of related organic–inorganic hybrid compounds. Two of them are Sn^{4+}-hybrid compounds containing discrete $[SnX_6]^{2-}$ (X = Cl, Br) octahedra surrounded by 2-chloroethylammonium cations (CSD refcodes KOVQOF, KOVQIZ; Elghoul *et al.*, 2024). The third compound is (2-bromoethylammonium)$_2$[SnBr$_6$] (USOTAB; Kreiman *et al.*, 2026), which is isostructural to the two mentioned above, while the fourth compound is (2-iodoethylammonium)$_2$[SnI$_4$], in which corner-sharing $[Sn^{II}I_6]^{4-}$ octahedra create infinite layers which are interleaved by organic cations (TEGROQ; Song *et al.*, 2022).

The title compound differs from these previously reported structures by containing Sn^{2+} cations and a *catena*-poly[tri-μ_2-bromidostannate(II)] inorganic substructure extending into infinite chains.

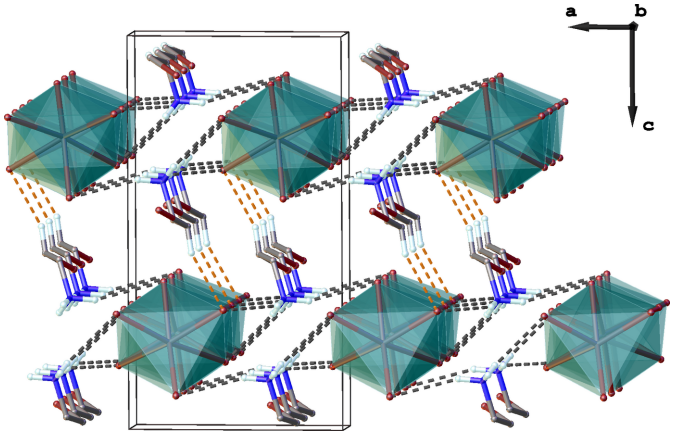

Figure 2
View of the inorganic chains propagating parallel to the *b* axis. N—H···Br interactions are shown as black dashed lines, C—H···Br bonds are shown as orange dashed lines. Disorder of the organic part and H atoms not involved in hydrogen-bonding interactions were omitted for clarity.

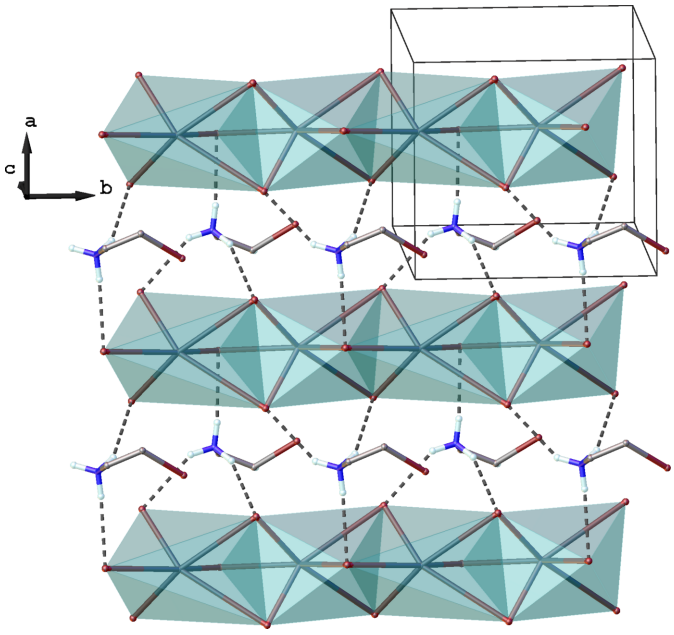

Figure 3
The supramolecular layer created by means of N—H···Br hydrogen bonds. Disorder of the organic part and H atoms not involved in hydrogen-bonding interactions were omitted for clarity.

5. Synthesis and crystallization

The title compound was obtained unintentionally upon the planned synthesis of (aziridinium)SnBr$_3$ by the vapor diffusion method; the single-crystal X-ray diffraction experiment established the formation of (2-BrC$_2$H$_4$NH$_3$)[SnBr$_3$] instead of the target perovskite. Tin(II) chloride (150 mg, 0.79 mmol, 1 eq.) was dissolved in 1 ml of water and 0.1 ml of hydrochloric acid (37% *w*/*w*) to avoid hydrolysis. To this solution 0.5 ml of ammonia solution (25% *w*/*w*) were added and stirred. As a result, a white precipitate of Sn(OH)$_2$ was formed. The precipitate was filtered off and washed with water. The obtained tin hydroxide was dissolved in a mixture of 2.4 ml of hydrobromic acid (48% *w*/*w*) and 4.5 ml of water. 0.2 ml of this acidic solution of tin(II) bromide was placed in a 1 ml vial. This vial was placed in a larger vial containing aziridine. The colourless crystals that formed within 1 h were collected immediately and kept in Paratone oil prior to measurements.

6. Refinement

Crystal data, data collection and structure refinement details are summarized in Table 3. The positional disorder of the organic cation was modelled over two set of sites, with C2 and Br4 atoms disordered over two positions and C1 and N1 atoms not being disordered. The sum of occupancies for disordered atoms was set to unity. The refined occupancies are 0.526 (18) and 0.474 (18) for parts *A* and *B*, respectively. H atoms were placed at calculated positions and refined with U_{iso}(H) = 1.2U_{eq}(C), U_{iso}(H) = 1.2U_{eq}(N). H atoms of secondary CH$_2$ groups were refined as riding, while H atoms of NH$_3^+$ groups were refined as rotating. The crystal under investigation was

found to be twinned by a 180° rotation around [100], and the intensity data processed into a HKLF5-type file; the twin components refined to a ratio of 0.6570 (11) : 0.3430 (11).

Acknowledgements

The authors are grateful to the FAIRE programme provided by the Cambridge Crystallographic Data Centre (CCDC) for the opportunity to use the Cambridge Structural Database (CSD) and associated software.

Funding information

Funding for this research was provided by: Ministry of Education and Science of Ukraine (grant No. 24BF037-02).

Table 3
Experimental details.

Crystal data	
Chemical formula	$(C_2H_7BrN)[SnBr_3]$
M_r	483.42
Crystal system, space group	Monoclinic, $P2_1/n$
Temperature (K)	200
a, b, c (Å)	7.883 (3), 8.7065 (6), 14.4937 (11)
β (°)	90.513 (13)
V (Å^3)	994.7 (4)
Z	4
Radiation type	Mo $K\alpha$
μ (mm^{-1})	18.56
Crystal size (mm)	0.12 × 0.06 × 0.02
Data collection	
Diffractometer	XtaLAB Synergy, Dualflex, HyPix
Absorption correction	Analytical [*CrysAlis PRO* (Rigaku OD (2024), using a multifaceted crystal model based on expressions derived by Clark & Reid (1995)]
T_{min}, T_{max}	0.184, 0.648
No. of measured, independent and observed [$I > 2\sigma(I)$] reflections	3899, 3899, 3101
R_{int}	0.034
$(\sin\theta/\lambda)_{max}$ (Å^{-1})	0.708
Refinement	
$R[F^2 > 2\sigma(F^2)]$, $wR(F^2)$, S	0.038, 0.087, 1.04
No. of reflections	3899
No. of parameters	94
H-atom treatment	H-atom parameters constrained
$\Delta\rho_{max}$, $\Delta\rho_{min}$ (e Å^{-3})	0.97, −0.69

Computer programs: *CrysAlis PRO* (Rigaku OD, 2024), *SHELXT* (Sheldrick, 2015*a*), *SHELXL* (Sheldrick, 2015*b*), *OLEX2* (Dolomanov *et al.*, 2009) and *publCIF* (Westrip, 2010).

References

Clark, R. C. & Reid, J. S. (1995). *Acta Cryst.* A**51**, 887–897.

Dolomanov, O. V., Bourhis, L. J., Gildea, R. J., Howard, J. A. K. & Puschmann, H. (2009). *J. Appl. Cryst.* **42**, 339–341.

Elghoul, A., Hajlaoui, F., Karoui, K., Allain, M., Mercier, N., Kozma, E., Botta, C. & Zouari, N. (2024). *New J. Chem.* **48**, 12235–12245.

Fabini, D. H., Laurita, G., Bechtel, J. S., Stoumpos, C. C., Evans, H. A., Kontos, A. G., Raptis, Y. S., Falaras, P., Van der Ven, A., Kanatzidis, M. G. & Seshadri, R. (2016). *J. Am. Chem. Soc.* **138**, 11820–11832.

Groom, C. R., Bruno, I. J., Lightfoot, M. P. & Ward, S. C. (2016). *Acta Cryst.* B**72**, 171–179.

Kreiman, D. S., Korytko, D. M., Kuzevanova, I. S., Dascalu, M. & Gural'skiy, I. A. (2026). *Acta Cryst.* E**82**, 1–4.

Kucheriv, O. I., Sirenko, V. Y., Petrosova, H. R., Pavlenko, V. A., Shova, S. & Gural'skiy, I. A. (2023). *Inorg. Chem. Front.* **10**, 6953–6963.

Li, W., Wang, Z., Deschler, F., Gao, S., Friend, R. H. & Cheetham, A. K. (2017). *Nat. Rev. Mater.* **2**, 16099.

Mantina, M., Chamberlin, A. C., Valero, R., Cramer, C. J. & Truhlar, D. G. (2009). *J. Phys. Chem. A* **113**, 5806–5812.

Pitaro, M., Tekelenburg, E. K., Shao, S. & Loi, M. A. (2022). *Adv. Mater.* **34**, 2105844.

Rigaku OD (2024). *CrysAlis PRO*. Rigaku Oxford Diffraction, Yarnton, England.

Sheldrick, G. M. (2015*a*). *Acta Cryst.* A**71**, 3–8.

Sheldrick, G. M. (2015*b*). *Acta Cryst.* C**71**, 3–8.

Shi, Y., Ma, Z., Zhao, D., Chen, Y., Cao, Y., Wang, K., Xiao, G. & Zou, B. (2019). *J. Am. Chem. Soc.* **141**, 6504–6508.

Sirenko, V. Y., Kucheriv, O. I., Shova, S. & Gural'skiy, I. A. (2024). *Mater. Today* **41**, 102452.

Song, Z., Yu, B., Wei, J., Li, C., Liu, G. & Dang, Y. (2022). *Inorg. Chem.* **61**, 6943–6952.

Spanopoulos, I., Hadar, I., Ke, W., Guo, P., Sidhik, S., Kepenekian, M., Even, J., Mohite, A. D., Schaller, R. D. & Kanatzidis, M. G. (2020). *J. Am. Chem. Soc.* **142**, 9028–9038.

Stoumpos, C. C., Mao, L., Malliakas, C. D. & Kanatzidis, M. G. (2017). *Inorg. Chem.* **56**, 56–73.

Tao, K., Li, Q. & Yan, Q. (2024). *Adv. Opt. Mater.* **12**, 2400018.

Westrip, S. P. (2010). *J. Appl. Cryst.* **43**, 920–925.

Zhang, L., Mei, L., Wang, K., Lv, Y., Zhang, S., Lian, Y., Liu, X., Ma, Z., Xiao, G., Liu, Q., Zhai, S., Zhang, S., Liu, G., Yuan, L., Guo, B., Chen, Z., Wei, K., Liu, A., Yue, S., Niu, G., Pan, X., Sun, J., Hua, Y., Wu, W., Di, D., Zhao, B., Tian, J., Wang, Z., Yang, Y., Chu, L., Yuan, M., Zeng, H., Yip, H., Yan, K., Xu, W., Zhu, L., Zhang, W., Xing, G., Gao, F. & Ding, L. (2023). *Nano-Micro Lett.* **15**, 1–48.

Zhou, C., Lin, H., He, Q., Xu, L., Worku, M., Chaaban, M., Lee, S., Shi, X., Du, M.-H. & Ma, B. (2019). *Mater. Sci. Eng. Rep.* **137**, 38–65.

supporting information

Acta Cryst. (2026). E**82**, 825-828 [https://doi.org/10.1107/S2056989026006079]

Crystal structure of *catena*-poly[2-bromoethylammonium [tin(II)-tri-μ-bromido]]

Valeriia M. Ovdenko, Mircea-Odin Apostu, Irina A. Golenya, Anna Yu. Myronenko and Il'ya A. Gural'skiy

Computing details

***catena*-Poly[2-bromoethylammonium [tin(II)-tri-μ-bromido]]**

Crystal data

$(C_2H_7BrN)[SnBr_3]$
M_r = 483.42
Monoclinic, $P2_1/n$
a = 7.883 (3) Å
b = 8.7065 (6) Å
c = 14.4937 (11) Å
β = 90.513 (13)°
V = 994.7 (4) Å^3
Z = 4
$F(000)$ = 864
D_x = 3.228 Mg m^{-3}
Mo $K\alpha$ radiation, λ = 0.71073 Å
Cell parameters from 2192 reflections
θ = 2.7–28.4°
μ = 18.56 mm^{-1}
T = 200 K
Plate, colourless
0.12 × 0.06 × 0.02 mm

Data collection

XtaLAB Synergy, Dualflex, HyPix diffractometer
Radiation source: micro-focus sealed X-ray tube, PhotonJet (Mo) X-ray Source
Mirror monochromator
Detector resolution: 10.0000 pixels mm^{-1}
ω scans
Absorption correction: analytical [CrysAlisPro (Rigaku OD (2024), using a multifaceted crystal model based on expressions derived by Clark & Reid (1995)]
T_{min} = 0.184, T_{max} = 0.648
3899 measured reflections
3899 independent reflections
3101 reflections with $I > 2\sigma(I)$
R_{int} = 0.034
θ_{max} = 30.2°, θ_{min} = 2.7°
h = −9→9
k = −11→11
l = −19→19

Refinement

Refinement on F^2
Least-squares matrix: full
$R[F^2 > 2\sigma(F^2)]$ = 0.038
$wR(F^2)$ = 0.087
S = 1.04
3899 reflections
94 parameters
0 restraints
Hydrogen site location: inferred from neighbouring sites
H-atom parameters constrained
$w = 1/[\sigma^2(F_o^2) + (0.0412P)^2 + 2.5221P]$ where $P = (F_o^2 + 2F_c^2)/3$
$(\Delta/\sigma)_{max} < 0.001$
$\Delta\rho_{max}$ = 0.97 e Å^{-3}
$\Delta\rho_{min}$ = −0.69 e Å^{-3}

Special details

Geometry. All esds (except the esd in the dihedral angle between two l.s. planes) are estimated using the full covariance matrix. The cell esds are taken into account individually in the estimation of esds in distances, angles and torsion angles; correlations between esds in cell parameters are only used when they are defined by crystal symmetry. An approximate (isotropic) treatment of cell esds is used for estimating esds involving l.s. planes.

Refinement. Refined as a 2-component twin.

Fractional atomic coordinates and isotropic or equivalent isotropic displacement parameters (Å²)

	x	*y*	*z*	U_{iso}*/U_{eq}	Occ. (<1)
Sn1	0.24506 (6)	0.50701 (5)	0.23958 (4)	0.02780 (14)	
Br1	0.00481 (9)	0.69436 (8)	0.31340 (6)	0.03191 (19)	
Br4A	0.7829 (14)	0.0021 (4)	0.4183 (3)	0.0494 (14)	0.526 (18)
Br4B	0.6922 (16)	−0.0059 (3)	0.4114 (2)	0.0475 (16)	0.474 (18)
Br2	0.21352 (9)	0.32682 (8)	0.39200 (6)	0.03210 (19)	
Br3	0.50363 (9)	0.65306 (8)	0.32387 (6)	0.02965 (18)	
N1	0.7777 (8)	0.3505 (7)	0.3497 (5)	0.0347 (15)	
H1A	0.723604	0.283201	0.311459	0.042*	
H1B	0.891835	0.337768	0.344926	0.042*	
H1C	0.749523	0.448271	0.333513	0.042*	
C1	0.7255 (14)	0.3215 (11)	0.4465 (7)	0.054 (2)	
H1AA	0.825780	0.333795	0.487421	0.065*	0.526 (18)
H1AB	0.641222	0.400138	0.464319	0.065*	0.526 (18)
H1BC	0.600418	0.329253	0.449890	0.065*	0.474 (18)
H1BD	0.774061	0.403046	0.486318	0.065*	0.474 (18)
C2A	0.656 (3)	0.176 (2)	0.4611 (16)	0.057 (7)	0.526 (18)
H2AA	0.542464	0.173121	0.430883	0.068*	0.526 (18)
H2AB	0.637669	0.163218	0.528206	0.068*	0.526 (18)
C2B	0.779 (3)	0.169 (2)	0.4840 (12)	0.035 (4)	0.474 (18)
H2BA	0.738155	0.159334	0.548165	0.042*	0.474 (18)
H2BB	0.904294	0.164162	0.485746	0.042*	0.474 (18)

Atomic displacement parameters (Å²)

	U^{11}	U^{22}	U^{33}	U^{12}	U^{13}	U^{23}
Sn1	0.0282 (3)	0.0231 (2)	0.0321 (3)	−0.00033 (18)	−0.0004 (2)	−0.0030 (2)
Br1	0.0244 (4)	0.0272 (4)	0.0441 (5)	0.0036 (3)	0.0027 (3)	0.0006 (3)
Br4A	0.065 (4)	0.0267 (10)	0.0565 (14)	0.0088 (13)	0.0095 (17)	0.0081 (8)
Br4B	0.068 (5)	0.0285 (10)	0.0456 (14)	−0.0016 (13)	0.0030 (16)	0.0022 (8)
Br2	0.0382 (4)	0.0246 (4)	0.0334 (4)	−0.0019 (3)	−0.0025 (3)	0.0024 (3)
Br3	0.0239 (3)	0.0280 (4)	0.0371 (5)	−0.0018 (3)	−0.0010 (3)	0.0008 (3)
N1	0.035 (3)	0.023 (3)	0.046 (4)	0.004 (2)	−0.002 (3)	−0.003 (3)
C1	0.082 (7)	0.038 (5)	0.042 (5)	0.009 (4)	0.015 (5)	−0.009 (4)
C2A	0.077 (16)	0.045 (11)	0.049 (13)	0.006 (10)	0.034 (12)	0.001 (10)
C2B	0.030 (10)	0.044 (10)	0.030 (9)	−0.003 (7)	−0.016 (8)	0.005 (7)

Geometric parameters (Å, º)

Sn1—Br1	2.7256 (10)	N1—C1	1.487 (11)
Sn1—Br2	2.7228 (9)	C1—H1AA	0.9900
Sn1—Br3	2.6869 (11)	C1—H1AB	0.9900
Sn1—Br2^{i}	3.3922 (9)	C1—H1BC	0.9900
Sn1—Br1^{ii}	3.4518 (10)	C1—H1BD	0.9900
Sn1—Br3^{ii}	3.7621 (9)	C1—C2A	1.40 (2)
Br4A—C2A	1.921 (19)	C1—C2B	1.49 (2)
Br4B—C2B	1.968 (19)	C2A—H2AA	0.9900
N1—H1A	0.9100	C2A—H2AB	0.9900
N1—H1B	0.9100	C2B—H2BA	0.9900
N1—H1C	0.9100	C2B—H2BB	0.9900
Br3—Sn1—Br2	88.75 (3)	N1—C1—H1AB	108.7
Br3—Sn1—Br1	93.74 (3)	N1—C1—H1BC	108.6
Br2—Sn1—Br1	87.56 (3)	N1—C1—H1BD	108.6
Br3—Sn1—Br2^{i}	77.92 (2)	N1—C1—C2B	114.5 (10)
Br2—Sn1—Br2^{i}	159.89 (3)	H1AA—C1—H1AB	107.6
Br1—Sn1—Br2^{i}	78.47 (3)	H1BC—C1—H1BD	107.6
Br3—Sn1—Br1^{ii}	92.40 (3)	C2A—C1—N1	114.2 (11)
Br2—Sn1—Br1^{ii}	77.44 (3)	C2A—C1—H1AA	108.7
Br1—Sn1—Br1^{ii}	163.66 (3)	C2A—C1—H1AB	108.7
Br2^{i}—Sn1—Br1^{ii}	117.66 (3)	C2B—C1—H1BC	108.6
Br3—Sn1—Br3^{ii}	152.91 (3)	C2B—C1—H1BD	108.6
Br2—Sn1—Br3^{ii}	71.04 (2)	Br4A—C2A—H2AA	108.0
Br1—Sn1—Br3^{ii}	102.93 (3)	Br4A—C2A—H2AB	108.0
Br2^{i}—Sn1—Br3^{ii}	125.98 (2)	C1—C2A—Br4A	117.2 (14)
Br1^{ii}—Sn1—Br3^{ii}	66.24 (3)	C1—C2A—H2AA	108.0
Sn1—Br1—Sn1^{i}	89.10 (3)	C1—C2A—H2AB	108.0
H1A—N1—H1B	109.5	H2AA—C2A—H2AB	107.2
H1A—N1—H1C	109.5	Br4B—C2B—H2BA	108.9
H1B—N1—H1C	109.5	Br4B—C2B—H2BB	108.9
C1—N1—H1A	109.5	C1—C2B—Br4B	113.5 (11)
C1—N1—H1B	109.5	C1—C2B—H2BA	108.9
C1—N1—H1C	109.5	C1—C2B—H2BB	108.9
N1—C1—H1AA	108.7	H2BA—C2B—H2BB	107.7
N1—C1—C2A—Br4A	51 (2)	N1—C1—C2B—Br4B	−58.2 (17)

Symmetry codes: (i) −*x*+1/2, *y*+1/2, −*z*+1/2; (ii) −*x*+1/2, *y*−1/2, −*z*+1/2.

Hydrogen-bond geometry (Å, º)

D—H···*A*	*D*—H	H···*A*	*D*···*A*	*D*—H···*A*
N1—H1*A*···Br1^{ii}	0.91	2.66	3.507 (7)	156
N1—H1*B*···Br2^{iii}	0.91	2.62	3.491 (6)	160
N1—H1*C*···Br3	0.91	2.64	3.425 (6)	145

C1—H1*BD*···Br2^{iv}	0.99	2.94	3.882 (9)	159
C2*A*—H2*AA*···Br2	0.99	2.97	3.85 (3)	149

Symmetry codes: (ii) −*x*+1/2, *y*−1/2, −*z*+1/2; (iii) *x*+1, *y*, *z*; (iv) −*x*+1, −*y*+1, −*z*+1.

Sn — Br bond length (Å) in coordination octahedron.

	Bond length (Å)
Sn1—Br1	2.7256 (10)
Sn1—Br2	2.7228 (9)
Sn1—Br3	2.6869 (11)
Sn1—Br1^{i}	3.4517 (10)
Sn1—Br2^{iv}	3.3923 (9)
Sn1—Br3^{i}	3.7621 (10)

Symmetry codes: (i) -x+1/2, y-1/2, -z+1/2; (iv) -x+1/2, y+1/2, -z+1/2